

GT2007-28351

## TURBINE INLET ICE RELATED FAILURES AND PREDICTING INLET ICE FORMATION

David M. Maas  
El Paso Corporation

Nathan M. McCown  
El Paso Corporation

### ABSTRACT

Ice ingestion has caused damage and subsequent failures of a Solar Mars 100 natural gas pipeline gas turbine on two separate occasions in Seligman Arizona. Understanding this phenomenon and the required ambient conditions is key to preventing ice related failures in the future. This paper investigates the required ambient temperature and relative humidity for inlet ice formation. It presents the data collected from an on site ambient temperature and relative humidity meter as well as a real time bell-mouth inlet camera.

An ambient temperature and relative humidity meter was installed on site and used to protect the turbine by shutting it down (trip) based on high relative humidity and low ambient temperatures. The initial criteria of relative humidity greater than 95% and ambient temperature less than 35.5°F (1.9°C) used to trip and protect the unit were a combination of an educated guess and values cited in General Electric document *Gas Turbine Inlet Air Treatment*. [1] To further refine these trip parameters and better understand the inlet icing process, a camera was installed in the turbine inlet housing with a view of the bell-mouth and inlet guide vanes (IGV). This provided real time images of the inlet icing phenomena that was then correlated with the ambient temperature and relative humidity (RH). Also, the camera images showed, after a significant icing event, that pieces of ice sloughed off the IGVs and were ingested by the turbine. Weather Radar data collected from [www.weather.com](http://www.weather.com) showed that this can occur without precipitation.

The theory of inlet ice formation was investigated using the Magnus equation for dew-point calculations and the "Ideal Gas Law" with an assumption of constant specific heat for the

flowing inlet temperature depression. Using a temperature recovery factor of 0.8 (this has been supported by numerical modeling in previous research by Stewart [2]) the inlet guide vane temperature depression was predicted to be 6.9°F (3.8°C). With this IGV temperature depression, icing was predicted for ambient temperatures less than 38.9°F (32+6.9°F) (3.8°C) and RH above 74 to 76%. Evidence is also given for inlet ice formation on a General Electric model Frame 3 turbine at the same location.

The collected RH, ambient temperature data and inlet camera images suggest condensate and not precipitate icing could be the root cause of the past ice ingestion failures.

With the ambient temperature, RH data and bell-mouth camera images, the temperature depression at the inlet guide vanes was measured to be about 9.5°F (5.3°C). The temperature recovery factor (RF) was shown to be 0.73. A 9.5°F (5.3°C) IGV temperature drop will result in IGV ice when ambient temperatures are below 41.5°F (32+9.5°F) (5.3°C) and RH above 67 to 69%. Setting the trip criteria to guarantee ice free operation will negatively impact the reliability and drop it to unacceptable levels. The original trip criteria of relative humidity greater than 95% and ambient temperature less than 35.5°F (1.9°C) remain and are now seen as an acceptable compromise.

Inlet air heating as a method of preventing inlet ice formation will be discussed. The amount of heat added to the inlet air to guarantee ice free operation is determined to be greater than 250 hp (186 kW). Finally, options for the inlet air heating energy source are suggested.

## 1.0 INTRODUCTION

The Seligman Arizona Solar Mars 100 turbine and compressor set has had two suspected ice ingestion related failures in the last three years; one in the spring of 2003 and again in the fall of 2004. The damage that caused both of these failures occurred during winter storm conditions; hence the suspected ice related failure. The total cost of these failures has been about \$203,000, with the vast majority spent on the 2004 failure. After the costly 2004 failure, a relative humidity (RH) meter was installed at Seligman station. A basic set of alarm and trip criteria were developed, based largely on engineering gut instinct and values cited in General Electric document *Gas Turbine Inlet Air Treatment*. [1]. Primarily, the conclusion that wall temperature depression at the inlet of LM2500 turbine was about 3°F (1.7°C). [1] The alarm and trip criteria were implemented on the Seligman Solar turbine and it had numerous ice formation alarms and trips during the remainder of the 2004/2005 winter.

On November 23, 2004 foggy conditions with ambient temperatures at or below freezing were present at Seligman station. The Mars unit was shut down and this photo was taken of the inlet guide vanes (IGV) with a hand held camera from an inlet duct access panel. This photo confirmed the suspected ice formation.



Figure 1. Proof of IGV Ice Formation

To further understand the formation of IGV ice, a camera was installed in the inlet duct work of the Seligman Mars and was set up to continuously record images of the IGVs while the turbine was running (see Fig 2). This camera successfully captured multiple icing events during the 2005/2006 winter. By analyzing these images with the trended ambient temperature and RH, the alarm and trip criteria can be more precisely defined. Also, the temperature depression at the inlet guide vanes can be calculated and compared to the established theory.

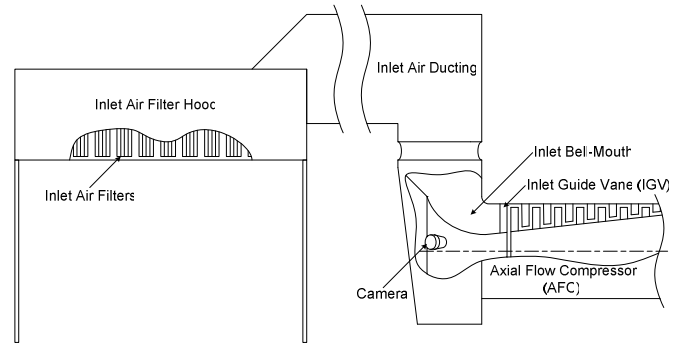


Figure 2. Inlet filter ducting, AFC Cross-Section, and Camera Placement

## 2.0 ICE INGESTION FAILURES

During the two suspected ice failures of the Seligman Mars turbine, the only logged atmospheric conditions were the ambient temperature. Winter storm conditions were verified by El Paso employees in the Seligman vicinity. Furthermore, this unit was installed in late 2001, so it has experienced relatively few winter storms while running.

### 2.1 MARCH 3<sup>RD</sup>, 2003 FAILURE

A high pitched noise was noted coming from the axial flow compressor (AFC) or gas producer (GP) of the Mars unit by the Cross Functional Technician responsible for Seligman Station the day after a winter storm on March 2<sup>nd</sup>. The situation was discussed with mechanical Services-North, and the unit was shut down. The initial bore scope inspection showed a bent first stage AFC blade. With the help of Solar technicians, one half of the AFC case was removed and four of the first stage blades were replaced (see Fig 3). The total cost was \$11,907.20 not including loss of throughput. [3]

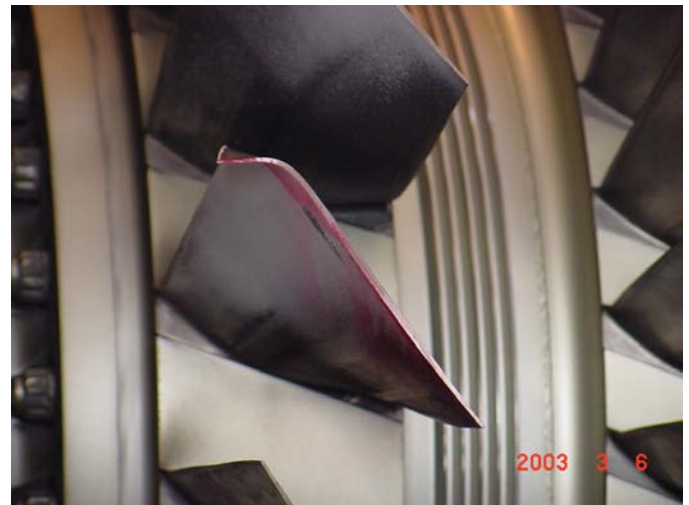


Figure 3. Bent First Stage AFC Blade

Upon inspecting the inlet ducting, some leaks were discovered. The initial conclusion was rain/sleet from the previous day's storm was sucked through these leaks and puddled in the bottom of the inlet ducting. At some point during the winter

weather, ambient conditions were cold enough for this water to freeze into large sheets that could break off and be sucked into the turbine inlet. This could have bent the first stage AFC blades.

A second similar theory was rain/sleet had been sucked through the inlet leaks and was collecting and freezing on the bell-mouth trash screen. The trash screen is wire mesh with half inch opening locked in the turbine bell-mouth. The trash screen would be several degrees cooler than the ambient air due to the inlet temperature depression. Under the right conditions the water leaking into the inlet ducting would freeze on contact with the screen. Over time the ice would build up and then large pieces could break off and be sucked into the first stage of the turbine and this could have bent the first stage AFC blades.

Both of these theories are examples of precipitation icing. [4] After this failure, all inlet air duct leaks were repaired.

## 2.2 NOVEMBER 9<sup>TH</sup>, 2004 FAILURE

On November 9<sup>th</sup>, 2004 the Seligman Mars turbine tripped off line on high vibration. On an attempted restart the unit sounded very poor and was immediately shut down. Previously on October 28<sup>th</sup>, 2004 an audible change was noted in the turbine, but was not severe enough to warrant action. Again, this change in the turbine operating sound occurred after a heavy snow storm.

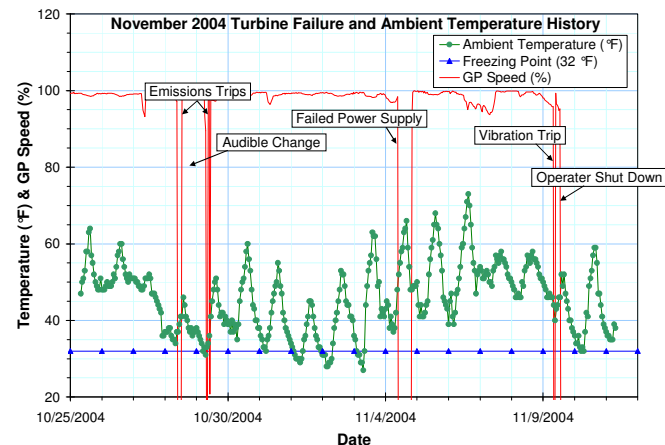


Figure 4. November 2004 Temperature History

On clear days and nights the ambient temperature has a large daily swing. High humidity and precipitation is indicated when there is a very small diurnal temperature variation. As the temperatures approach freezing, the rain will change to sleet or snow, as was the case on the 27<sup>th</sup> and 28<sup>th</sup> of October. The failure and ambient history can be seen in Fig. 4.

On November 19<sup>th</sup>, 2004 the Solar Mars 100 AFC was torn down with the help of Solar technicians. This time, damage from possible ice ingestion was severe; one of the first stage AFC blade tips had broken off and gone through the turbine (see Fig 5). This damaged multiple blades and stators in successive stages in the AFC.



Figure 5. Broken First Stage AFC Blade Tip

It is suspected that ice ingestion caused a bent AFC blade tip or tips and the resultant change in the turbine operating sound on October 28<sup>th</sup>. The turbine then continued to run until one of the bent blade tips fatigue failed and went through the AFC. The result was a \$191,320.95 repair bill not including loss of throughput.

This second failure was puzzling since the inlet filter and ducting had been well sealed less than two years earlier and it didn't seem possible for liquid water to make its way to the turbine inlet. Nonetheless ice still appeared to be the likely cause of the damage.

## 3.0 INSTRUMENTATION & SETUP

There were two basic instruments which were used to gather the data needed for this project, a temperature/RH meter and a day/night security camera.

### 3.1 RELATIVE HUMIDITY METER

A Johnson Controls HT-6703 Outdoor Humidity Transmitter was selected to monitor relative humidity as well as ambient temperature. The Transmitter Provided a 4-20 mA signal to the Allen Bradley PLC5 40E processor for both the humidity and temperature.

### 3.2 CAMERA

A low cost security camera was chosen for the project. The benefit of a day/night security camera is the onboard infrared light source (LEDs). This camera was not only cost efficient but also supplied sufficient resolution for ice detection on the IGVs. A Video Web Server and associated software was also supplied with the camera. This server was assigned an IP address and was used to access the live video of the turbine inlet and guide vanes via the company intranet.

There were some issues with installing a camera in a Class I Division 2 environment. Explosion proof video cameras are available but were far too large, as well as very expensive. The security camera was made explosion proof by placing it in

Class I Division 2 housing. A window faced Rosemount transmitter housing accepted the camera nicely and is already Class I Division 2 certified. To minimize fogging on the inside of the housing window, a few packages of silica gel were placed inside.

The Camera was placed inside of the bell housing on the inlet air ducting approximately 2 ½ feet from the leading edge of the first stage set of variable pitch inlet guide vane stators. There was one necessary consideration for this installation, the camera needed to be outside of the trash screen located in the center of the bell housing. During the first test run of the camera, the glare of the light emitted from the camera's LEDs on the screen was so intense that the inlet guide vanes were not visible. The decision was made to cut a small hole in the trash screen approximately the size of the window on the Rosemount housing. This provided a well lit, glare free view of the inlet guide vanes.

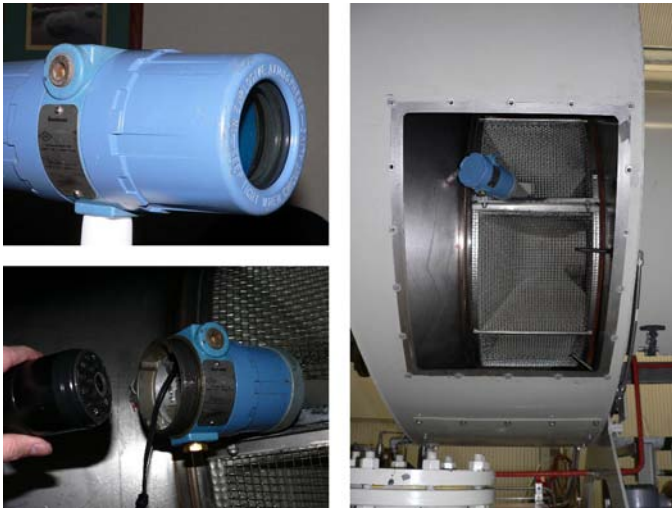


**Figure 6. Window Faced Rosemount Housing, Camera, and Camera Mounting**

The inlet Camera and its housing will cause some degree of inlet flow distortion and turbulence. There was no modeling or calculations done to determine the degree of flow disruption or its effect on the turbine AFC blades. The decision was made to keep the camera on the outside of the trash screen with the thought that it would be “far enough” from the turbine inlet. The bearing vibration monitors were monitored when the turbine was started for the first time with the camera in place. There was no noticeable change in the vibration signal pre and post camera installation. Additionally, the Seligman Mars 100 has 6000 plus hours of run time with the camera in place without incident. So it has since been concluded that the Camera induced inlet flow distortion and turbulence did not detrimentally affect the turbine AFC Blades.

### 3.3 SIGNAL PROCESSING AND DATA LOGGING

The ambient air temperature and relative humidity signals that are driven to the PLC by the ambient temperature and RH transmitter had a lot of natural fluctuation. This fluctuation

would have caused the turbine to trip unnecessarily when the data reached the alarm and trip set points. These set points are as follows: Alarm at 36.5°F (2.5°C) and RH at 90%, Trip at 35.5°F (1.9°C) and below with RH being at 95% and above. To alleviate these unnecessary trips, a first order digital filter was added to the logic to allow for sudden and short changes in the relative humidity and ambient temperature (which happens frequently at the Seligman location) without tripping the turbine. The ambient air temperature signal filter uses a 15 minute (900 second) time constant and the RH signal uses a 30 (1800 second) minute time constant. Refer to Fig. 7. The filtered signals were logged for the 2005/2006 winter. The raw signals were added to logger for the 2006/2007 winter.

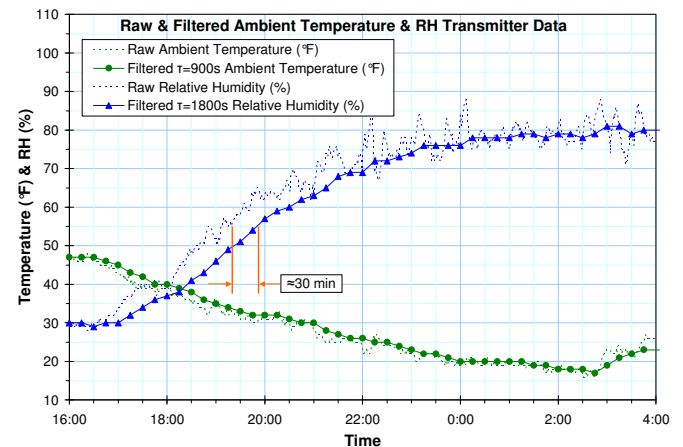


**Figure 7. Raw & Filtered Ambient Temperature & RH Transmitter Data**

### 3.4 VIDEO WEB SERVER IMAGE LOGGING

The Video Web Server and supplied software was used to log the image stream on a remote computer. The band width of the Video Web Server's IP address was narrowed to limit the video stream to 1 frame every 5 seconds. This kept the data storage requirements to a minimum, but more than sufficient for this project.

### 4.0 THEORY

For water to form on a surface such as an IGV, the surface and the air immediately adjacent to the surface need to be at or below the dew point temperature. The dew point is a function of the ambient temperature and RH. If the dew-point temperature is above the freezing point then water will condense on the surface. If the dew-point temperature is below the freezing point ice will form on the surface.

The air entering the bell-mouth of a turbine has been accelerated to a high velocity by the AFC induced pressure depression. At the IGVs, the velocity is on the order of 500 ft/s (341 mph, 152 m/s). [2] This causes a temperature depression at the IGVs that is several degrees below ambient. So the IGV surface can be below the freezing point, and at or below the dew-point temperature, even when the ambient conditions are well above 32°F (0°C) and below 100% RH.

#### 4.1 DEW POINT & RELATIVE HUMIDITY

The relative humidity (RH) of air is the ratio of the partial pressure of the water vapor in the air with respect to the saturation partial pressure of water vapor over a flat surface of pure water. [5]

$RH$  = Relative humidity (%)

$p_w$  = Partial Pressure of Water Vapor (psia)

$p_{ws}$  = Saturation Partial Pressure of Water Vapor (psia)

$$RH = 100 p_w / p_{ws} \quad (1)$$

**Relative Humidity (RH) Formula [6]**

“The dew-point temperature is the temperature to which the air must be cooled to reach saturation (assuming air pressure remains the same). When the temperature cools to the dew point, fog or dew can occur, and the relative humidity becomes 100%.”. [7] The dew-point temperature can be calculated from the Magnus formula and parameters. The Magnus parameters are valid from -49°F to 140°F (-45°C to 60°C).

$$\beta = 17.62$$

$$\lambda = 243.12$$

$RH$  = Relative Humidity (%)

$T_a$  = Ambient Temperature (°C)

$T_d$  = Dew-Point Temperature (°C)

$$T_d = \frac{\lambda \left( \ln \left( \frac{RH}{100} \right) + \frac{\beta T_a}{\lambda + T_a} \right)}{\beta - \left( \ln \left( \frac{RH}{100} \right) + \frac{\beta T_a}{\lambda + T_a} \right)} \quad (2)$$

**Magnus Dew-Point Formula [8]**

#### 4.2 BELL-MOUTH TEMPERATURE & PRESSURE DEPRESSION

The AFC inlet mass flow of a Solar Mars 100 turbine is 91.0 lb<sub>m</sub>/s (41.3 kg/s). [9] Using the Ideal Gas Law at ISO standard conditions of 59°F, 14.696 psia (15°C, 1 atm) and inlet cross-sectional area of 1.84 ft<sup>2</sup> (0.171 m<sup>2</sup>) with the IGVs fully open, the inlet velocity is calculated to be 646 ft/s (441 mph, 197 m/s). This represents the air flow at rated AFC speed; since it is proportional to actual volumetric flow it is independent of ambient temperature and pressure within the context of the Ideal Gas Law. The acceleration of the inlet air from zero to 646 ft/s (197 m/s) causes a drop in temperature. If the acceleration into the inlet bell-mouth occurs adiabatically, (this has been supported by numerical modeling [2]), then the temperature depression is simply a result of conservation of energy. Air temperature is traded for velocity.

$c_p$  = 186.72 ft·lb<sub>f</sub>/lbm·°F (1.004 kJ/kg·K) Specific Heat of

Air at 40°F (4.4°C)

$g$  = 32.2 ft/s<sup>2</sup> (9.81 m/s<sup>2</sup>) Standard Acceleration of Gravity

$T$  = Static or Bell-Mouth Flowing Temperature (°F)

$T_0$  = Stagnation or Ambient Temperature (°F)

$V$  = Bell-Mouth Flowing Velocity (ft/s)

$$T_0 = T + \frac{V^2}{2c_p g} \quad (3)$$

**Stagnation Temperature Formula [2]**

The temperature depression ( $\Delta T$ ) from the ambient to the flowing temperature in the bell-mouth is 34.7°F (19.3°C) when calculated with a bell-mouth velocity of 646 ft/s (197 m/s). If the inlet flow to the turbine is assumed to be isentropic the pressure depression at the bell-mouth can be calculated. The calculated bell-mouth pressure depression is about 2.7 psi (18.6 kPa).

$k$  = 1.4 Specific Heat Ratio for Air

$P$  = Static or Bell-Mouth Flowing Pressure (psia)

$P_0$  = Stagnation or Ambient Pressure (psia)

$T$  = Static or Bell-Mouth Flowing Temperature (R)

$T_0$  = Stagnation or Ambient Temperature (R)

$$\frac{P_0}{P} = \left( \frac{T_0}{T} \right)^{k/(k-1)} \quad (4)$$

**Stagnation Pressure Formula [6]**

The air velocity immediately adjacent to the surface of the IGVs is at or nearly at zero as dictated by boundary conditions. Therefore the air near the IGV surface has recovered most of its initial ambient temperature. This temperature recovery can be quantified by the recovery factor (RF) and previous research has shown to be about 0.8. [2]

$RF$  = 0.8 Recovery Factor

$T$  = Static or Bell-Mouth Flowing Temperature (°F)

$T_0$  = Stagnation or Ambient Temperature (°F)

$T_{RFC}$  = Recovery Factor Corrected Temperature (°F)

$$RF = \frac{(T_{RFC} - T)}{(T_0 - T)} \quad (5)$$

**Recovery Factor Formula [2]**

The inlet guide vane surface temperature depression is calculated at 6.9°F (3.8°C) when using a bell-mouth flowing  $\Delta T$  of 34.7°F (19.3°C) and a RF of 0.8. The RF corrected temperature can then be used to calculate the recovered



pressure at the leading edge of the IGVs and show that it is about 0.58 psi (4.0 kPa) below the ambient pressure.

#### 4.3 WALL TEMPERATURE EQUATION

The temperature of inlet surfaces can also be calculated by the wall temperature equation given in the Solar document, *The Application Guidelines for Treatment of Turbine Inlet Air* [4]

$k = 1.4$  Specific Heat Ratio for Air

$M = 0.6$  Mach Number for 646 ft/s (197 m/s) Air Velocity @ 40°F (4.4°C)

$P_N = 0.72$  Prandtl Number

$T_0$  = Ambient Temperature (K)

$T_w$  = Wall Temperature (K)

$$T_w = T_0 - T_0 \left( 1 - \sqrt{P_N} \right) \left( 1 - \frac{2}{M^2(k-1) + 2} \right) \quad (6)$$

Wall Temperature Formula [4]

The inlet surface (wall) temperature using this Eq. (6) can be calculated. Using an air velocity of 646 ft/s (197 m/s) and an ambient temperature of 40°F (4.4°C) the surface temperature is 34.9°F (1.6°C). This is a  $\Delta T$  of 5.1°F (2.8°C) and of similar magnitude to the value of 6.9°F (3.8°C) calculated in section 4.2. Both of these calculations are approximations and contain a fudge factor, the Prandtl number in the wall temperature equation and the recovery factor used in Eq. (5).

#### 4.4 PREDICTING IGV ICING CONDITIONS

Using the predicted IGV surface temperature depression of 6.9°F (3.8°C) from section 4.2 the dew-point temperature at the IGVs can be calculated across a range of ambient temperatures and relative humidity.

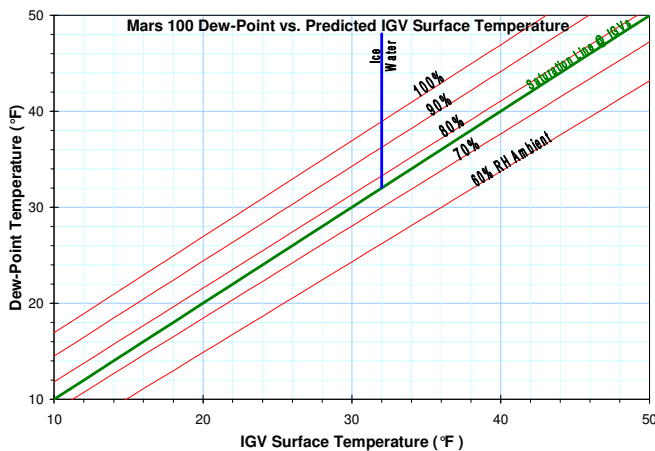


Figure 8. Dew-Point vs. Predicted IGV Surface Temperature

Notice that when the ambient RH has reached 74 to 76%, the saturation temperature has been reached at the IGVs. This is a result of the predicted  $\Delta T$  of 6.9°F (3.8°C). Ice is predicted to form on the inlet guide vanes at ambient temperatures below 38.9°F (32+6.9°F) (3.8°C) and RH above 74 to 76%. The reason for the RH range is the constant RH lines are not exactly parallel with the saturation line (see Fig. 8).

#### 4.6 DATA COLLECTION ERROR & UN-FILTERING CORRECTION

The initial reason for installing an ambient RH and temperature transmitter at Seligman station was to provide some means of protecting the turbine. The actual RH signal was heavily filtered with a 30 minute time constant first order filter. This was to keep from repeatedly crossing the trip criteria of 95% RH during an icing event. The filtered data was logged and the true un-filtered data was not. This was a mistake since the actual RH and the time of its occurrence is needed to determine the moment of ice first forming on the IGVs. To approximate the true RH value at a given time, an un-filtering algorithm can be applied to the filtered data that was logged. This was not required for the ambient temperature data, even though it was filtered with a first order filter and time constant set at 15 minutes. Figure 7 shows the error between the true ambient temperature data and filtered data is small, but this is not the case for the RH data.

The transfer function  $G(s)$  for a first order filter can be used to calculate an un-filtering algorithm.

$s$  = Complex Variable

$\tau = 1800$ (sec) The Time Constant

$$G(s) = \frac{\tau}{s + (1/\tau)} \quad (7)$$

Transfer Function for a First Order Filter [10]

Whenever the filtered RH signal is changing at roughly a constant rate, it can be approximated as a linear time domain function. This is usually the case after sunset as the ambient RH rises and the temperature drops, and sunrise as the ambient RH drops and temperature increases. The transfer function for a first order filter response to a linear time domain signal such as  $r(t) = mt$  is shown in Eq. (8).

$m$  = Slope of Linear Time Domain Signal (RH/sec)

$$C(s) = \frac{m}{s^2} \frac{\tau}{s + (1/\tau)} \quad (8)$$

First Order Filter Response to a Linear Ramp of Slope  $m$  [10]

$t$  = Time (sec)

$$c(t) = m(t - \tau + \tau e^{-t/\tau}) \quad (9)$$

Time Domain Equivalent of Eq. (8) [10]

$$c(t) = m(t - \tau) \quad (10)$$

Steady State Equivalent of Eq. (9) [10]

Equation (9) is the complete time domain response of a first order filter to a linear time domain signal. The limit of Eq. (9) as  $t$  goes to infinity (the steady state response) is Eq. (10) and is simply the original linear signal  $r(t) = mt$  time shifted by the filter time constant,  $\tau$ .

The point of this Laplacian treatment shows that when the logged filtered RH is increasing approximately linearly, the un-filtered value can be approximated by time shifting the filtered values back by  $\tau$  or 30 minutes. This algorithm can be applied to roughly recover the unfiltered or actual relative humidity during periods of increasing or decreasing RH. The time shift between the un-filtered and filtered data can be seen in Fig. 7.

## 5.0 COLLECTED IMAGES & DATA

The turbine inlet camera images, weather radar images, ambient temperature values, and RH values were logged continuously during the 2005/2006 winter. There were 25 separate icing events recorded during this period. Images of ice first forming on the IGVs, images when peak RH occurred, and any others of particular significance were saved for each of the 25 separate icing events. The beginning of an icing event was determined by comparing a base image with no ice to one when ice just begins to form. Notice the ice first starting to form on the IGV in Fig. 10 compared to the base photo Fig. 9.

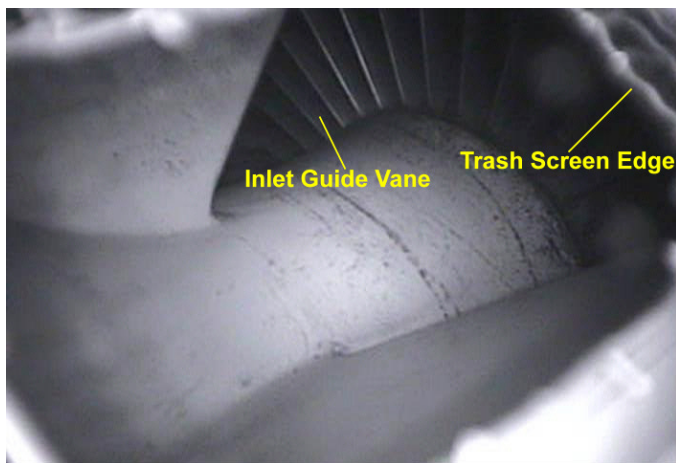


Figure 9. Base Photo of IGVs with No Ice

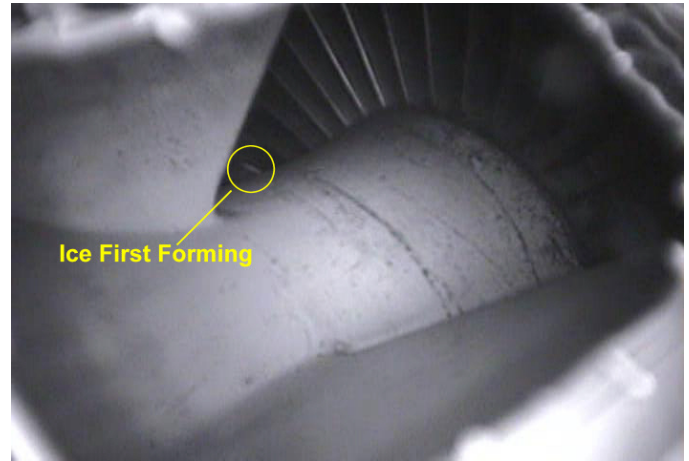


Figure 10. Photo of IGV Ice First Forming

## 5.1 ICING EVENT 01/01/2006 SAMPLE DATA (CLEAR CONDITIONS)

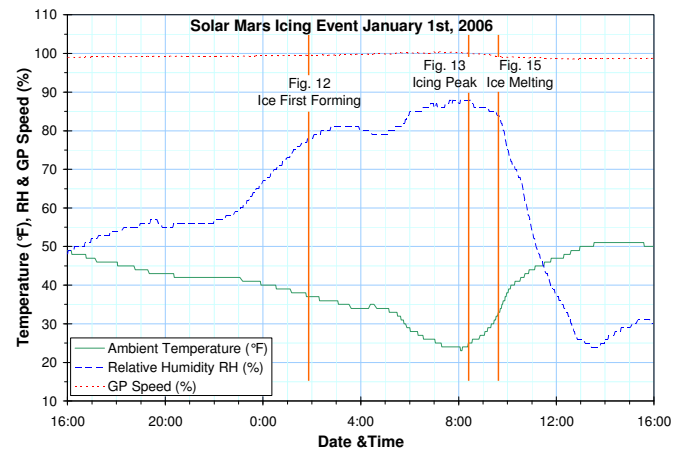
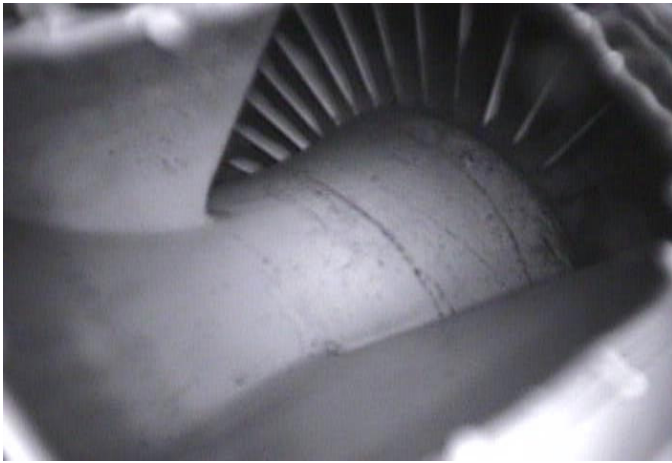


Figure 11. Icing Event 01/01/2006 Temperature & RH Trend



Figure 12. Ice First Forming 01/01/2006 01:51 @ 37°F (2.8°C) & 78% RH



**Figure 13. Icing Peak 01/01/2006 08:23 @ 24°F (-4.4°C) & 88% RH**

The weather radar map for this icing event shows clear conditions over Seligman Station, therefore precipitation being sucked through filters or leaks in the inlet duct work is not the source of the moisture. The IGV ice in Figures 12 & 13 is most evident when comparing them to the ice free base Fig. 9.



**Figure 14. Weather Radar Map 01/01/2006 08:24 [www.weather.com]**

Notice in Fig. 11 how quickly the ambient temperature rises. If you look at Fig. 15, only about an hour after the peak icing conditions were reached, you can see how quickly the ice is melting. Also note the jagged edges of the ice on the IGVs indicating pieces had broken off and been sucked through the AFC. Figure 11 shows the ambient temperature at 32°F and RH at 84% but changing rapidly. It must be remembered that both these values are influenced by a first order filter so the true ambient temperature is greater the 32°F (0°C) and the true RH is less than 84%.

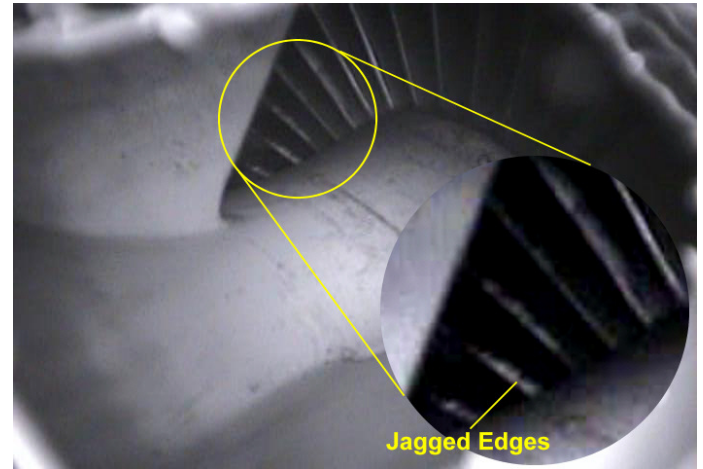


**Figure 15. Ice Melting 01/01/2006 09:38 @ 32°F (0°C) & 84% RH**

## 5.2 ICING EVENT 03/10/2006 SAMPLE DATA (WINTER STORM CONDITIONS)

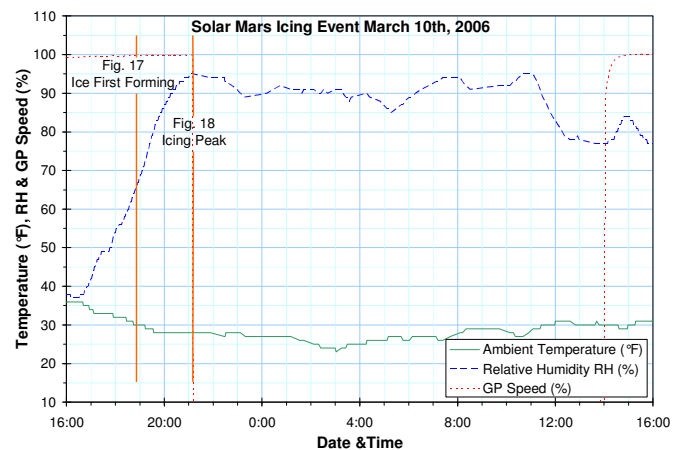


**Figure 16. Icing Event 03/10/2006 Temperature & RH Trend**



**Figure 17. Ice First Forming 03/10/2006 18:44 @ 30°F (-1.1°C) & 64% RH**



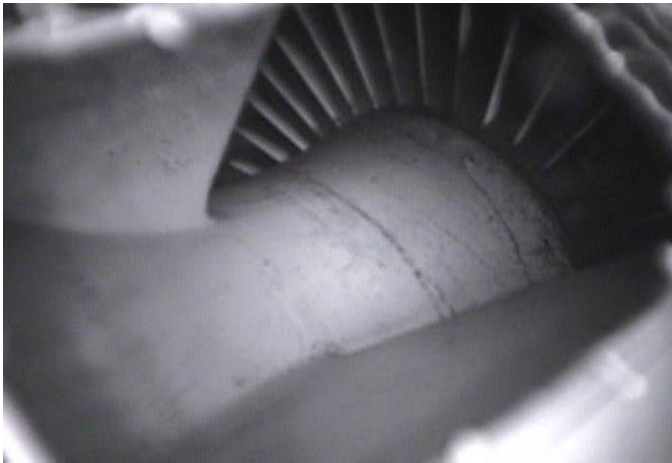


**Figure 18. Icing Peak 03/10/2006 21:08 @ 28°F (-2.2°C) & 95% RH**

The weather radar for this icing event shows a winter storm over Seligman Station. The ambient conditions reached the trip criteria of above 95% RH and below 35.5°F air temperature. The unit was shut down to prevent any ice ingestion damage.



**Figure 19. Weather Radar Map 03/10/2006 21:03**  
[www.weather.com]

### 5.3 DOES ICING OCCUR ON OTHER TURBINES?

The General Electric (GE) Frame 3 turbine at Seligman station was down for maintenance on 03/16/2006. The photo in Figure 20 was taken at this time. March 16<sup>th</sup> was only 6 days after a major storm had caused multiple icing events on the Mars unit only 100 yards away from the GE. In theory, the clean spots on the leading edge of the IGVs could be from ice formation and its subsequent melting, cleaning off the dirt. The IGVs were cleaned in March before the turbine was reassembled.



**Figure 20. GE Frame 3 Turbine Inlet Guide Vanes at Seligman Station 03/16/2006**

Figure 21 shows the IGVs at the end of August in 2006 after a summer with no icing conditions present. In this image, the leading edges of the IGVs are dirty, in theory because no ice has formed and melted to keep them clean. This supports the theory that inlet guide vane ice also forms on the GE at Seligman station and likely any turbine in climates where the ambient temperature approaches freezing.



**Figure 21. GE Frame 3 Turbine Inlet Guide Vanes at Seligman Station 08/30/2006**

The GE has been in place for 20 plus years and has never experienced an ice ingestion failure. It is equipped with a vane type inertial filter. [1] The inlet filter on this unit is at best in poor condition and likely has multiple leaks. The filter housing is equipped with bypass doors that are sucked open if the pressure drop across the filter element is too large. Under winter storm conditions these doors have been observed in there open position for extended periods of time.

## 6.0 ANALYSIS

The collected data can be used to show the IGV icing is the result of condensate icing or precipitate icing. Also, the images of ice first forming that were captured with each icing event can be used to calculate the temperature depression  $\Delta T$  at the inlet guide vanes. Finally, data collected during icing events can be displayed on a dew-point versus measured IGV surface temperature plot.

### 6.1 CONDENSATE ICING OR PRECIPITATE ICING?

The Solar document, *The Application Guidelines for Treatment of Turbine Inlet Air* [4], describes condensate icing as moisture containing air that is cooled to its dew-point by the inlet temperature depression. If this temperature depression is below freezing then ice will form on inlet surfaces. Precipitate icing is caused by liquid water entering the inlet system through the filters or leaks during precipitation weather events. This water then makes its way to the turbine bell-mouth and the inlet temperature depression causes it to freeze. The density of condensate ice is substantially less than that of precipitate ice. [4]

The inlet camera captured images of ice forming on the inlet guide vanes during cold clear nights. This can be seen in the sample data set in section 5.1. The weather conditions were clear and precipitation free as shown on the weather radar map in Fig. 14. Thus, this set of data is the result of condensate icing and not precipitate icing. In fact, the majority of the ice events captured by the inlet camera were on cold clear nights. Additionally, when the ambient conditions warmed and the IGV ice started to melt, the photos show IGV ice with jagged edges showing the condensate ice was thick enough to break off in chunks and enter the AFC. (see Fig. 15)

Images captured during a winter storm do not show any liquid or frozen water up stream of the IGVs. (see Section 5.2) Primarily I would expect to see ice collecting on the edges of the trash screen visible in Fig. 18 if liquid water was making its way into the inlet ducting, but I do not. This supports the conclusion that icing during a winter storm is also condensate ice and not caused by water being drawn through the inlet filter or leaky inlet ducting (precipitate ice). IGV ice which formed under rain, sleet or snowing conditions shows the same jagged edges when the ice melts with rapidly warming ambient temperatures at the end of the storm. The difference between a winter storm icing event and cold clear night icing event, is the duration and the higher relative humidity. Both of these conditions could cause thicker ice formation and thus larger pieces when they break off.

### 6.2 IGV TEMPERATURE DEPRESSION & RF

The camera allowed the tracking of the ambient temperature and RH the moment ice began to form on the IGVs. By calculating the dew point temperature when ice first starts to form, the IGV surface temperature can be inferred and the actual inlet guide vane temperature depression can be measured.

The moment of first ice formation was estimated from the captured images during each icing event. The time stamp was then used to retrieve the associated ambient temperature and RH from the trended data. Since the RH data was filtered with a digital first order filter, the RH values had to be corrected per the algorithm described in section 4.6. The dew-point for each pair of ambient temperature and corrected RH values was calculated and this represented the temperature of the IGVs at that moment. The difference, with respect to the ambient temperature, was the IGV temperature depression, at that moment. The average IGV temperature depression was measured to be 9.5°F (5.3°C).

The theory in section 4.2 predicted the IGV temperature depression of 6.9°F (3.8°C) with a RF 0.8. This also predicted ice formation at ambient temperatures below 38.9°F (3.8°C) and relative humidity above 74 to 76%. Using the measured temperature depression of 9.5°F (5.3°C), the actual RF for the IGVs of Mars 100 is 0.73. This gives ice formation criteria of ambient temperatures below 41.5°F (32+9.5°F) (5.3°C) and RH levels above about 67 to 69%. Again, there is a range of RH values because the lines of constant relative humidity are not quite parallel with the saturation line.

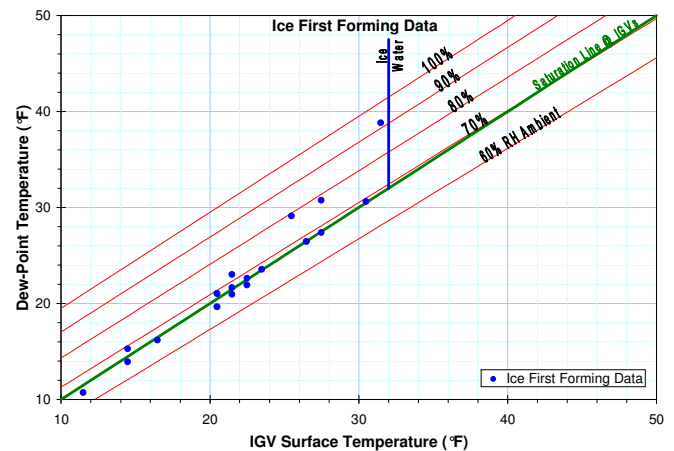
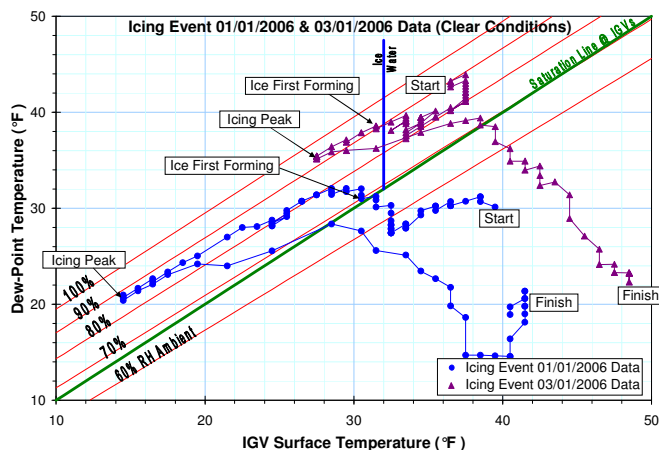


Figure 22. Ice First Forming Data

The ice first forming dew-point versus IGV surface temperature data has been plotted in Fig. 22. They cluster around the saturation line when the IGV temperature is below freezing or 41.5°F (5.3°C) ambient and the ice/water (freezing) line when IGV temperature is above 32°F (0°C). The data points should fall exactly on the saturation and freezing line but don't due to the error in determining the exact moment of ice formation from the inlet camera image stream and the error in correcting the filtered RH data.

An individual icing event can be shown on the same dew-point versus IGV surface temperature plot (see Fig. 23).



**Figure 23. Icing Event 01/01/2006 & 03/01/2006 Plot (Clear Conditions)**

The changing ambient conditions create a track that starts in a non icing region of the plot and approaches the saturation or freezing line as the ambient temperature drops at night. IGV ice forms as the track crosses the saturation line below the freezing point or crosses the freezing line above the saturation line. On clear cold nights with RH above 67 to 69%, the icing peak is reached just before sunrise after which the ambient temperatures climb rapidly and the data tracks back into non-icing regions. At this point, the ice collected on the IGVs either sublimates or melts away. Figure 15 shows the IGV ice from the January 1<sup>st</sup> 2006 event, melting, breaking into pieces and being sucked into the AFC.

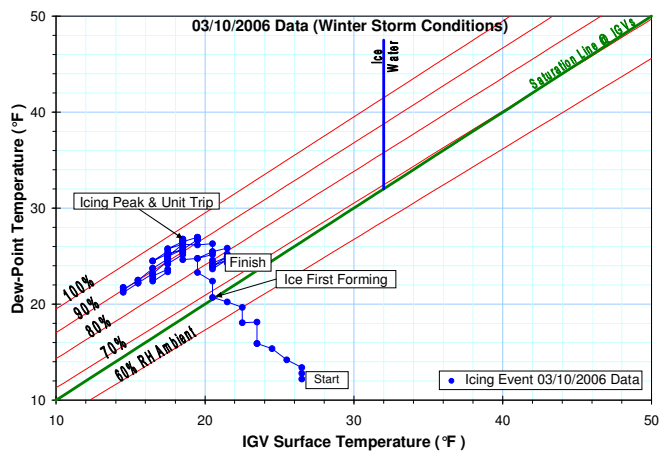


**Figure 24. Icing Event 03/10/2006 Plot (Winter Storm Conditions)**

In Fig. 24 is data from a winter storm event and again the changing ambient conditions create track. As the winter storm approaches, the track crosses the saturation line just as ice begins to form on the IGVs. The unit trips off line about an hour later when the ambient RH reached the trip point of 95%. The winter storm keeps the track on the left side of the saturation line for the remainder of the next day with RH in the mid 90's.

## 6.3 SOURCES OF ERROR

- The velocity profile of bell-mouth inlet flow was assumed to be constant when in reality there will be some areas of higher flow than others.
- Estimating the exact moment of ice formation from the inlet camera image stream.
- Correcting the filtered RH values to approximate the true RH values. The unfiltered data should have been logged as well.
- Ambient temperature and relative humidity measurement error of  $\pm 0.55^\circ\text{F}$  ( $0.31^\circ\text{C}$ ) and  $\pm 3\%$  accordingly.

## 7.0 PREVENTING IGV ICE FORMATION

Heating the inlet air reduces its relative humidity and increases the maximum ambient (before the air is heated) RH that is required for ice to form on the IGVs. Heating the inlet air stream will also lower the minimum temperature for icing to occur. Using the Mars 100 as an example, the theory developed in section 4 and the IGV temperature depression measured as described in section 6, can be used to calculate how adding heat to the inlet air flow will change the icing criteria. Starting with an inlet volumetric flow rate of 71400 cfm ( $33.6 \text{ m}^3/\text{s}$ ) the icing criteria for different quantities of inlet heat can be calculated.

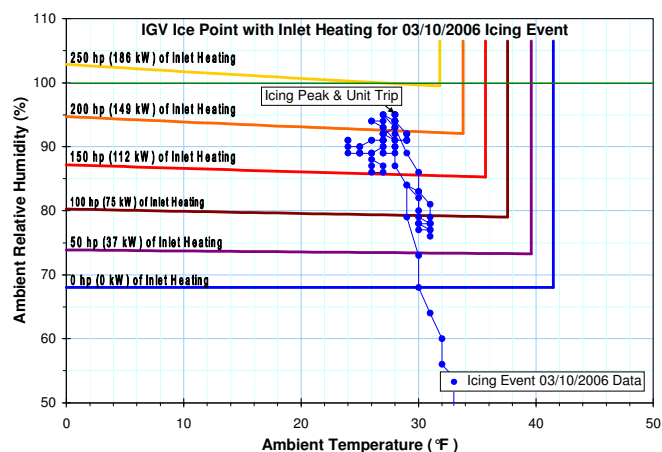


**Figure 25. IGV Ice Point with Inlet Air Heating for 03/10/2006**

The blue, zero, inlet heat line in Fig. 25, is the measured icing criteria of above 68% RH and ambient temperatures below  $41.5^\circ\text{F}$  ( $5.3^\circ\text{F}$ ) without inlet heating. The successive lines above this represent different amounts of heat added to the inlet air flow. The energy added to the inlet air is cast in the units of horse power to give a sense of scale with respect to a 11,400 hp (8,500 kW) site rated turbine. It should also be noted that the 250 hp (186 kW) line just crosses the 100% RH level. This implies that adding a little more than 250 hp (186 kW) worth of heat will guarantee ice free operation of the turbine. Once the inlet air is heated to the point the water

vapor partial pressure needed for 68% RH after heating is greater than the water vapor saturation pressure at ambient temperatures (before heating) condensation on the IGVs is not possible. There is simply not enough water present at any extremes of ambient temperatures.

The icing event that tripped the Mars 100 offline on March 10<sup>th</sup> is also displayed on the IGV ice point plot with inlet heating (see Fig. 25). The ambient conditions track shows about 225 hp (168 kW) of inlet heating would have kept ice from forming on the IGVs for the March 10<sup>th</sup> winter storm.

## 7.1 METHODS OF INLET HEATING

- Bleeding air off one of the later stages of the AFC back into the inlet ducting.
- Recirculating a portion of the exhaust gasses back into the inlet ducting.
- Passing fresh air over a heat exchanger with exhaust gasses flowing through it.
- Passing fresh air through the oil coolers and into the inlet ducting.
- Using electric resistive heaters in the inlet ducting.

These are merely a sample of the many ways to achieve inlet air heating. All systems will affect turbine performance by simulating a warmer day. Any system that uses energy from within the gas firing cycle or dilutes the available oxygen at the turbine inlet will have an additional impact on the performance. Exhaust gas recirculation will likely effect turbine wear, maintenance intervals, and emissions. Any system considered for a Mars 100 will have to meet the energy demands given in Figure 25.

## 8.0 TURBINE FAILURE CONCLUSIONS

The March 3<sup>rd</sup>, 2003 failure may have been the result of a leaky inlet duct and precipitate icing. However, it is possible the November 9<sup>th</sup>, 2004 failure was the result of condensate icing. The filter housing and inlet ducting had previously been well sealed, limiting the moisture source to only water vapor which formed as condensate ice on the IGVs. Without the RH and ambient temperature trips in place, the turbine was allowed to run until the condensate ice build up was sufficiently thick enough to slough off the IGVs and damage the first stage AFC blades.

The inlet camera does not show any liquid or frozen water up stream of the IGVs during storming conditions. This supports the conclusion that moisture source for the November 9<sup>th</sup>, 2004 failure was condensate ice.

The inlet camera does show that when IGV ice melts, it sometimes does so in an uneven jagged manner, indicating pieces are being sucked into the first stage AFC blades. None of the logged icing events, since the camera installation, have caused any damage. Therefore, none of the ice that was imaged, was thick enough or broke off in large enough chunks to damage the AFC blades. However, since the installation of

the inlet camera the turbine is limited to operate only when the RH is below 95% and the ambient temperature is greater than 35.5°F (1.9°C). It is possible condensate ice caused the November 9<sup>th</sup>, 2004 failure.

## 8.1 IGV ICE FORMATION CONCLUSIONS

Ice will form on the IGVs of a Solar Mars 100 turbine when the relative humidity is above 67 to 69% and the ambient temperature is below 41.5°F (5.3°C). It is likely ice will form on the inlet guide vanes of a turbine in any location where ambient temperatures approach the freezing point. This is supported by evidence that a GE Frame 3 turbine in the same location also experiences inlet guide vane icing.

The initial icing trip criteria of above 95% RH and below 35.5°F (1.9°C) ambient will not guarantee ice free operation. However, setting the criteria to 68% (67 to 69%) RH and 41.5°F (5.3°C) to trip the turbine will guarantee ice free operation, but will also negatively impact reliability in the winter months. So the original trip criteria remain.

Heating the inlet air will extend the range of ambient conditions a turbine can run without IGV icing and is quantified in Figure 25. Adding little over 250 hp (186 kW) of heat to the inlet air will guarantee ice free operation.

## 8.2 HOW MUCH ICE?

How much ice does it take to damage a Mars? It seems reasonable after looking at images of ice first forming on the IGVs that this small amount would not damage the turbine, and allowing some level of ice formation is not detrimental. Also, Fig. 15 shows pieces of ice were breaking off the IGVs and being sucked through AFC, but no damage was recorded at any time during the 2005/2006 winter. Had there been damage, the inlet camera system did not have the resolution to gauge the thickness of the ice on the IGVs. We simply don't know how much ice it takes to damage a Mars 100, but it has occurred in the past.

The Vibro-Meter is a sensor that can measure the thickness of ice build up on a small diaphragm. It measures the change in resonate frequency of the vibrating diaphragm as ice accumulates on its surface and converts this value to an output signal that is a function of ice thickness. The Vibro-Meter diaphragm is placed in the turbine bell-mouth close to the IGVs any ice build occurs on both. [11] This device is being considered for ongoing experimentation.

## ACKNOWLEDGMENTS

The authors would like thank the El Paso Natural Gas Flagstaff Area Operations, for supporting field research. Also, Danena Meza is thanked for her efforts in editing this document.



## REFERENCES

- [1] Loud, R.L., & A.A. Slaterpryce (undated). *Gas Turbine Inlet Air Treatment*, GER-3419A. Schenectady, NY: General Electric Company.
- [2] Stewart, W.E., Jr. 2000. Air Temperature Depression and Potential Icing at the Inlet of Stationary Combustion Turbines. *ASHRAE Transactions* 106(2): 318-327.
- [3] Lazos, M., Jr. 2003. *Gas Turbine Engine Repair Report Seligman C*. El Paso Corporation.
- [4] Johnson, R.S. (undated). *Applications Guidelines for Treatment of Turbine inlet Air*. San Diego, CA: Solar Turbines Incorporated, Subsidiary of Caterpillar Inc.
- [5] Babin, S.M. 2000. *Water Vapor Myths: A Brief Tutorial*. <http://fermi.jhuapl.edu/people/babin/vapor/index.html>.
- [6] Çengel, Y.A. & M.A. Boles, 1998. *Thermodynamics An Engineering Approach*, Third Edition. Boston: McGraw-Hill.
- [7] Sensirion, (undated). *SHTxx Application Note Dew-Point Calculation*. <http://www.gas-flow-sensor.com/images/getFile?id=83#search=%22SHTxx%20Application%20Note%20Dew-Point%20Calculation%22>. Stäfa, ZH Switzerland: Sensirion Ag.
- [8] Sonntag D. 1990. Important New Values of the Physical Constants of 1986, Vapour Pressure Formulations Based on the IST-90 Psychrometer Formulae. *Z. Meteorol.*, 70(5), pp. 340-344.
- [9] Solar Turbines, (undated). *Mars 100 Gas Turbine Compressor Set*. <http://mysolar.cat.com/cda/files/126854/7/ds100cs.pdf>. San Diego, CA: Solar Turbines Incorporated, Subsidiary of Caterpillar Inc.
- [10] Phillips, C.L. & R.D. Harbor, 2000. *Feedback Control Systems, Fourth Edition*. Upper Saddle River, NJ: Prentice Hall, pp. 117-121.
- [11] Vibro-Meter SA, (undated). *Ice Detection System for Gas Turbine: EW 140 Ice Sensor DIC 413 De-Icing Controller*. <http://www.vibro-meter.com/industrial/sensors-other.html>. Rte Moncor 4 P.O. Box CH-1701 Fribourg, Switzerland: Vibro-Meter SA.
- Hardy, B. 1998. ITS-90 Formulations for Vapor Pressure, Frostpoint Temperature, Dewpoint Temperature, and Enhancement Factors in the Range -100 to 100 C. *The Proceedings of the Third International Symposium on Humidity & Moisture*. Teddington, London, England.
- Johnson Controls, 2001 *Hx-67x3 Series Outdoor Relative Humidity Transmitter Product Bulletin*, LIT-120181. Milwaukee, WI: Johnson Controls, Inc.
- Stewart, W.E., Jr. 2001. Condensation and Icing in Gas Turbine Systems: Inlet Air Temperature and Humidity Limits. *ASHRAE Transactions: Symposia*. pp. 887-891.